View this PDF in Utopia Documents for more interactive functionality
Download FREE software now

Biochem. J. (2015) **469**, 135–144 doi:10.1042/BJ20141330

The motor function of *Drosophila melanogaster* myosin-5 is activated by calcium and cargo-binding protein dRab11

Huan-Hong Ji*†, Hai-Man Zhang*†, Mei Shen*, Lin-Lin Yao* and Xiang-dong Li*[1]

*Group of Cell Motility and Muscle Contraction, State Key Laboratory of Integrated Management of Insect Pests and Rodents, Institute of Zoology, Chinese Academy of Sciences, Beijing 100101, China

†University of Chinese Academy of Sciences, Beijing 100049, China

In the *Drosophila melanogaster* compound eye, myosin-5 (DmM5) plays two distinct roles in response to light stimulation: transport of pigment granules to the rhabdomere base to decrease light exposure and transport of rhodopsin-bearing vesicles to the rhabdomere base to compensate for the rhodopsin loss during light exposure. However, little is known of how the motor function of DmM5 is regulated at the molecular level. In the present study, we overexpressed DmM5 in Sf9 insect cells and investigated its regulation using purified proteins. We found that the actin-activated ATPase activity of DmM5 is significantly lower than that of the truncated DmM5 having the C-terminal globular tail domain (GTD) deleted, indicating that the GTD is the inhibitory domain. The actin-activated ATPase activity of DmM5 is significantly activated by micromolar levels of calcium. DmM5 associates with pigment granules and rhodopsin-bearing vesicles through cargo-binding proteins Lightoid (Ltd) and dRab11 respectively. We found that GTP-bound dRab11, but not Ltd, significantly activates DmM5 actin-activated ATPase activity. Moreover, we identified Gln^{1689} in the GTD as the critical residue for the interaction with dRab11 and activation of DmM5 motor function by dRab11. Based on those results, we propose that DmM5-dependent transport of pigment granules is directly activated by light-induced calcium influx and the DmM5-dependent transport of rhodopsin-bearing vesicle is activated by active GTP-bound dRab11, whose formation is stimulated by light-induced calcium influx.

Key words: actin, ATPase, *Drosophila melanogaster* eye, molecular motor, rhabdomere, Rab11.

INTRODUCTION

Myosin is a type of molecular motor protein which converts energy from ATP hydrolysis into mechanical movement along actin filaments. Class V myosin (Myo5) is so far the best characterized unconventional myosin in term of cellular function and molecular regulation. Myo5 is widely expressed in almost all eukaryotes and implicated in trafficking and tethering a number of vesicles [1,2].

Vertebrates contain three genes of Myo5 (Myo5a, 5b and 5c), whereas *Drosophila melanogaster* has a single Myo5 gene, encoding *Drosophila* Myo5 heavy chain (DmM5). Like vertebrate Myo5, DmM5 contains the motor domain (residues 1–772), six IQ motifs (residues 773–916), several segments of coiled coil (CC; residues 917–1395) and the C-terminal globular tail domain (GTD, residues 1396–1792) (Figure 1A). Two identical heavy chains of DmM5 are dimerized through the CC region to form a homodimer. Although the overall structure of DmM5 is identical to that of Myo5a, their motor properties are quite different. It was reported that, unlike vertebrate Myo5a, DmM5 is a non-processive motor, which is unable to transport vesicles as a single molecule, but might participate in organelle transport by being present in ensembles [3].

The motor function of Myo5a is regulated by Ca^{2+} and cargo-binding proteins. A tail-inhibition mechanism for the regulation of Myo5a is now well accepted, i.e. Myo5a in the inhibited state is in a folded conformation such that the GTD interacts with and inhibits the motor activity [4–9]. High Ca^{2+} or cargo binding may reduce interaction between the GTD and motor domains, thus activating motor activity [4,7,8,10]. However, little is known about the regulation of DmM5.

In the *Drosophila* compound eye, DmM5 plays at least two distinct roles in sensory adaptation and in photoreceptor development and maintenance. When the fly eye is exposed to bright light, the pigment granules located in the photoreceptor cell cytoplasm move rapidly to the cytoplasmic face of the photosensitive membrane organelle, the rhabdomere and change the colour of the eye from dark red to bright green, which is called the deep pseudopupil phenomenon [11]. DmM5 couples Lightoid (Ltd) to transport pigment granules to the base of rhabdomere [12]. In mature photoreceptors, light induces elevation of cytosolic free Ca^{2+} and triggers DmM5/Ltd-dependent migration of pigment granules to the cytoplasmic face of rhabdomere, thus reducing rhodopsin exposure to light [12]. It is proposed that *in vivo* Ca^{2+} stimulates the motor function of DmM5 [12]. However, little is known about Ca^{2+} regulation of DmM5 motor activity at molecular level.

The second role played by DmM5 in *Drosophila* compound eye is the transport of secretory vesicles containing rhodopsin to the rhabdomere base in photoreceptor development and maintenance [13,14]. Two *Drosophila* proteins, dRab11 and dRip11 (the dRab11-interacting protein), also participate in secretory transport [13,15,16]. It has been shown that Rab11, the vertebrate counterpart of dRab11, binds to the GTD of Myo5b [17,18].

Abbreviations: CaM, calmodulin; CC, coiled coil; dCaM, *Drosophila* calmodulin; DmM5, *Drosophila* myosin-5; DmM5-FL, full-length DmM5; DmM5-1IQ, DmM5 containing the motor domain and IQ1; DmM5-motor, DmM5 containing the motor domain only; GEF, guanine-nucleotide-exchange factor; GTD, C-terminal globular tail domain of DmM5; GTPγS, guanosine 5′-[γ-thio]triphosphate tetralithium salt; HMM, heavy meromyosin; Ltd, lightoid; Mlc-C, *Drosophila* cytoplasmic myosin light chain; Myo5, myosin-5; RT, reverse transcription; RTW, rhabdomere terminal web; Sm-849, recombinant smooth muscle myosin S1.

[1] To whom correspondence should be addressed (email lixd@ioz.ac.cn).

© 2015 Authors; published by Portland Press Limited

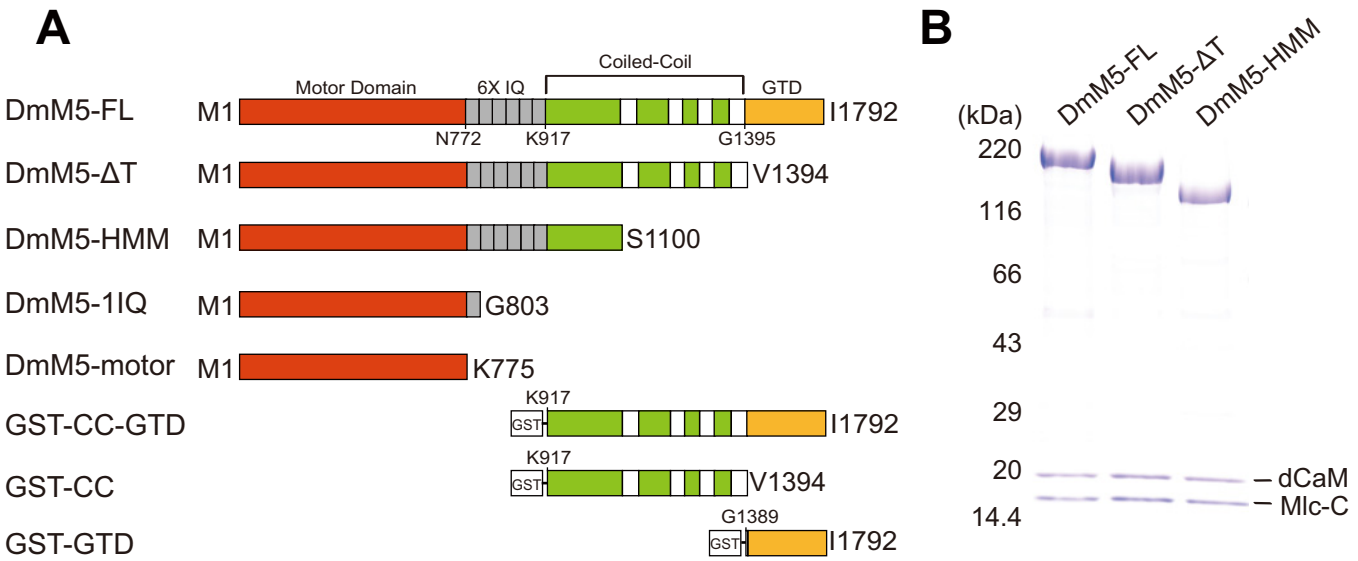

Figure 1 Schematic diagram of DmM5 constructs

(**A**) Schematic primary structure of DmM5 constructs. IQ represents the dCaM and Mlc-C-binding site. (**B**) SDS/PAGE of purified DmM5 constructs. The co-purified light chains dCaM and Mlc-C are indicated.

Since the GTD not only serves as a cargo-binding site but also functions as an inhibitory domain, we expected that Rab11 and dRab11 might interfere with the inhibitory function of the GTD, thus activating the motor function.

In the present study, we investigated the regulation of DmM5 using recombinant DmM5 and the associated proteins. We found that the actin-activated ATPase activity of DmM5 was stimulated by Ca^{2+} and cargo-binding protein dRab11, but not by cargo-binding protein Ltd.

EXPERIMENTAL

Materials

AccuScript Reverse Transcriptase and PfuUltra II Fusion HS DNA Polymerase were from Stratagene. Oligonucleotides were synthesized by Invitrogen. Restriction enzymes and modifying enzymes were purchased from New England Biolabs. Actin was prepared from rabbit skeletal muscle acetone powder according to Spudich and Watt [19]. Anti-Flag M2 antibody, anti-Flag M2 affinity gel, phosphoenolpyruvate, 2,4-dinitrophenyl-hydrazine, pyruvate kinase and glutathione were from Sigma–Aldrich. Flag peptide (D-Y-K-D-D-D-D-K) was synthesized by AuGCT. Glutathione–Sepharose 4 Fast Flow was from GE Healthcare.

Cloning, expression and purification of *D. melanogaster* myosin-5 constructs

The cDNA of DmM5 (GI: 4092802) was reverse-transcribed from *D. melanogaster* adult total RNA using AccuScript Reverse Transcriptase and amplified by PCR with primers 5′-TACGGTCGACATGTCTAGCGAGGAGATGC-3′ (underlined is the SalI site) and 5′-TGCAACTAGTATGGCAAA GTTCTCGACC-3′ (underlined is the SpeI site). The PCR product was cloned into pFastBacHFTc vector {a modified baculovirus transfer vector pFastBacHTc (Invitrogen) as described in [4]} using SalI and SpeI sites. The truncated constructs of DmM5 were created by introducing a stop codon at the indicated positions (Figure 1A). Q1689A mutation of DmM5-FL (full-length DmM5) was introduced by QuikChange site-directed mutagenesis with Pfu Ultra DNA Polymerase. The cDNAs generated by PCR were confirmed by sequencing. All DmM5 constructs contain an N-terminal Flag tag. Recombinant baculoviruses were prepared using Bac-To-Bac system (Invitrogen) as described previously [5].

To express recombinant DmM5, Sf9 insect cells were co-infected with the recombinant viruses encoding DmM5 heavy chain, *D. melanogaster* calmodulin (dCaM) and *Drosophila* cytoplasmic myosin light chain (Mlc-C). The expressed DmM5 was purified by anti-Flag M2 affinity chromatography as described previously [5].

To determine the protein concentrations of DmM5 constructs, we separated DmM5 samples along with serial dilutions of protein standard by SDS/PAGE (4–20 % gel). The protein bands were visualized by Coomassie Brilliant Blue staining and quantified using NIH ImageJ 1.42Q. Recombinant smooth muscle myosin S1 (Sm-849) was used as standard for protein concentration determination. Sm-849 was overexpressed in Sf9 cells and purified as described previously [20]. The molar concentration of Sm-849 was determined by absorbance at 280 nm using a molar absorption coefficient of 103 980 $l \cdot mol^{-1} \cdot cm^{-1}$ and its protein concentration was calculated based on its molecular mass of 102.78 kDa. The molar concentration of DmM5 was calculated based on following molecular masses (in kDa): 212.28 (DmM5-FL), 166.34 (DmM5-ΔT), 132.12 [DmM5-HMM (heavy meromyosin)], 96.03 (DmM5-1IQ), 93.15 (DmM5-motor).

To prepare GST-tagged DmM5 tail constructs (Figure 1A), the cDNAs of the constructs were cloned into pGEX4T1 using BamHI and XhoI sites. Point mutations were introduced by QuikChange site-directed mutagenesis. The constructs were expressed in *Escherichia coli* BL21(DE3) cells and purified with glutathione–Sepharose according to standard procedures. The purified GST-fusion proteins were dialysed against 10 mM Tris/HCl (pH 7.5), 0.2 M NaCl and 1 mM DTT at 4 °C overnight. The concentrations of GST-fusion proteins were measured by absorbance at 280 nm using the following molar absorption coefficients ($l \cdot mol^{-1} \cdot cm^{-1}$):

© 2015 Authors; published by Portland Press Limited

104 660 for GST–CC–GTD, 64 300 for GST–CC and 81 520 for GST–GTD.

Expression and purification of DmM5-associated proteins

dCaM was expressed and purified as described previously [21]. The cDNA of Mlc-C (GI: 17530801) was obtained by reverse transcription (RT)–PCR from *D. melanogaster* adult total RNA and cloned into pFastBac transfer vector (Invitrogen) and pT7-7 bacterial expression vector respectively. Mlc-C was purified as described for smooth muscle myosin light chain [22]. After dialysis against 30 mM Tris/HCl (pH 7.5), 30 mM NaCl and 1 mM DTT, Mlc-C was divided into aliquots and stored at − 80 °C. Protein concentrations were determined by absorbance at 280 nm using molar absorption coefficients ($l \cdot mol^{-1} \cdot cm^{-1}$) of 1280 for dCaM and 5360 for Mlc-C.

The cDNAs of dRab11 (GI: 2313039), dRip11 (GI: 7293490) and Ltd (GI: 17933630) were amplified by RT–PCR from *D. melanogaster* adult total RNA and cloned into pFastBacHFT transfer vectors. The procedures of recombinant baculovirus preparation and protein expression and purification were similar as described for DmM5. Before performing function assays, dRab11 or Ltd was incubated with a 3–5-fold molar excess of GDP (Amresco) or GTPγS (guanosine 5′-[γ-thio]triphosphate tetralithium salt; Millipore) and 3–5-fold molar excess of $MgCl_2$ for 30 min at 25 °C.

ATPase assay

The ATPase activity of DmM5 was measured in a plate-based ATP-regeneration system as described previously with slight modification [6]. Unless otherwise indicated, the ATPase activity of DmM5 in EGTA conditions was measured in a solution containing 20 mM MOPS/KOH (pH 7.0), 200 mM NaCl, 1 mM $MgCl_2$, 1 mM DTT, 0.25 mg/ml BSA, 15 μM dCaM and 15 μM Mlc-C, 0.5 mM ATP, 2.5 mM phosphoenolpyruvate, 20 units/ml pyruvate kinase, 100–200 nM DmM5, 80 μM actin and 1 mM EGTA at 25 °C. For the ATPase assay in Ca^{2+} conditions, 1 mM $CaCl_2$ was added and EGTA (1 mM) was adjusted to 0.87, 1.03, 1.41 and 5.06 mM for pCa4, pCa5, pCa6 and pCa7 respectively.

Actin co-sedimentation assay

The interaction between DmM5 and dRab11 was analysed by actin co-sedimentation as described previously [23]. Briefly, 0.8 μM DmM5 and 2.5 μM GTPγS–dRab11 were incubated with 4 μM actin in a 40 μl of solution containing 20 mM MOPS/KOH (pH 7.0), 150 mM NaCl, 1 mM $MgCl_2$, 1 mM EGTA, 8 μM dCaM and 8 μM Mlc-C on ice for 1 h. The mixtures were centrifuged at 418 000 ***g*** (Beckman Optima MAX-XP, TLA-120.1 rotor) for 15 min at 4 °C. To the supernatant, 10 μl of 5× SDS/PAGE loading buffer was added. The pellets were washed once with 120 μl of 20 mM MOPS/KOH (pH 7.0), 150 mM NaCl, 1 mM $MgCl_2$ and 1 mM EGTA and resuspended in 50 μl of 1× SDS/PAGE loading buffer. The pellets and the supernatants were subjected to SDS/PAGE (4–20 % gel) and visualized by Coomassie Brilliant Blue staining or Western blotting using the horseradish peroxidase (HRP)-conjugated anti-Flag M2 antibody.

GST pull-down assay

GST pull-down of GST-tagged DmM5 constructs with Flag-tagged GTPγS–Ltd was performed as follows. One hundred microlitre of 0.5 μM GST or GST-tagged proteins and 1.5 μM Flag-tagged GTPγS–Ltd in buffer A (20 mM MOPS/KOH, pH 7.0, 100 mM NaCl, 1 mM $MgCl_2$, 3 μM GTPγS, 1 mM EGTA and 1 mM DTT) was incubated with 15 μl of glutathione–Sepharose with rotation at 4 °C for 1 h. After washing with 100 μl of buffer A three times to remove the unbound proteins, the bound proteins were eluted with 39 μl of 100 mM Tris/HCl, pH 8.0, 20 mM GSH, 100 mM NaCl and 1 mM DTT, subjected to SDS/PAGE (4–20 % gel) and visualized by Coomassie Brilliant Blue staining and Western blot using anti-GST or anti-Flag antibody.

GST pull-down of GST-tagged DmM5 constructs with Flag-tagged GTPγS–dRab11 was performed as follows. One hundred microlitres of 1.5 μM GST or GST-tagged protein in PBS (137 mM NaCl, 2.7 mM KCl, 10 mM Na_2HPO_4 and 2 mM KH_2PO_4, pH 7.4) was first bound to 10 μl of glutathione–Sepharose and then incubated with 100 μl of 2 μM Flag-tagged GTPγS–dRab11 in buffer A. After washing away the unbound proteins with 100 μl of buffer A, the bound proteins were eluted with 39 μl of 20 mM GSH in 100 mM Tris/HCl (pH 8.0), subjected to SDS/PAGE (4–20 %) and visualized by Coomassie Brilliant Blue staining or Western blotting using anti-GST or anti-Flag antibody.

RESULTS

Expression and purification of DmM5

DmM5 heavy chain contains six IQ motifs, the binding sites for calmodulin (CaM) or CaM-like light chain. It has been shown that both *Drosophila* CaM (dCaM) and Mlc-C are the light chains of DmM5 [3]. Therefore, we co-expressed DmM5-FL with dCaM and Mlc-C in Sf9 cells. The expressed proteins were purified with anti-Flag affinity chromatography. DmM5 truncated constructs, including DmM5-ΔT (having the GTD domain deleted) and DmM5-HMM (having the medial CC and GTD domain deleted), were prepared similarly (Figure 1A). SDS/PAGE showed that the purified DmM5 constructs had molecular mass as expected from their amino acid sequence and associated stoichiometrically with dCaM and Mlc-C (Figure 1B).

Ca^{2+} stimulates the ATPase activity of DmM5

To examine whether the motor function of DmM5 is affected by Ca^{2+}, we measured the actin-activated ATPase activity (hereafter referred to as ATPase activity, unless otherwise indicated) of DmM5-FL in the presence of various concentrations of Ca^{2+}. As shown in Figure 2(A), Ca^{2+} significantly stimulated the ATPase activity of DmM5-FL. In EGTA conditions, DmM5 had relatively low ATPase activity (1.12 ± 0.15 head$^{-1} \cdot s^{-1}$), which is gradually increased with increasing of free Ca^{2+} concentration from pCa7 to pCa4. In pCa4 conditions, the ATPase activity of DmM5-FL was 2.92 ± 0.16 head$^{-1} \cdot s^{-1}$, ∼2.6-fold as that in EGTA conditions.

The ionic strength dependence of DmM5 ATPase activity is similar to that of vertebrate Myo5a [4,7]. With NaCl concentration increased from 50 to 500 mM, the ATPase activity of DmM5-FL in pCa4 gradually decreased and that in EGTA showed a bell-shape (Figure 2B). In the presence of 500 mM NaCl, the ATPase activities of DmM5-FL in pCa4 and EGTA conditions were roughly equal.

To further characterize the effects of Ca^{2+} on DmM5 ATPase activity, we examined the actin dependence of DmM5 ATPase activity in the presence of 50 mM NaCl in EGTA and pCa4 conditions. As shown in Figure 2(C) and Table 1, both the maximal ATPase activity (V_{max}) and the apparent

© 2015 Authors; published by Portland Press Limited

Table 1 Steady-state kinetic parameters of DmM5 ATPase activity

ATPase activities were measured as described in the legend to Figures 2(C) and 5(C). All data are means ± S.D. from three or four independent assays. The number in parentheses indicates the number of independent assays.

Constructs		Conditions	V_0 (head^{-1}·s^{-1})	V_{max} (head^{-1}·s^{-1})	K_{actin} (μM)
	EGTA	50 mM NaCl	0.19 ± 0.03 (4)	1.26 ± 0.19 (4)	40.9 ± 17.1 (4)
		200 mM NaCl	0.55 ± 0.05 (3)	2.12 ± 0.37 (3)	134.7 ± 36.4 (3)
DmM5-FL		200 mM NaCl + 15 μM dRab11	0.69 ± 0.05 (4)	4.34 ± 0.18 (4)	104.6 ± 17.6 (4)
	pCa4	50 mM NaCl	0.47 ± 0.03 (3)	2.59 ± 0.27 (3)	11.8 ± 1.9 (3)
		200 mM NaCl	0.70 ± 0.04 (3)	3.75 ± 0.88 (3)	79.8 ± 29.6 (3)
	EGTA	50 mM NaCl	0.51 ± 0.07 (3)	5.45 ± 0.70 (3)	23.6 ± 4.2 (3)
DmM5-HMM		200 mM NaCl	0.48 ± 0.11 (4)	5.75 ± 0.79 (4)	72.1 ± 5.7 (4)
	pCa4	50 mM NaCl	0.49 ± 0.05 (4)	2.83 ± 0.14 (4)	12.4 ± 3.4 (4)

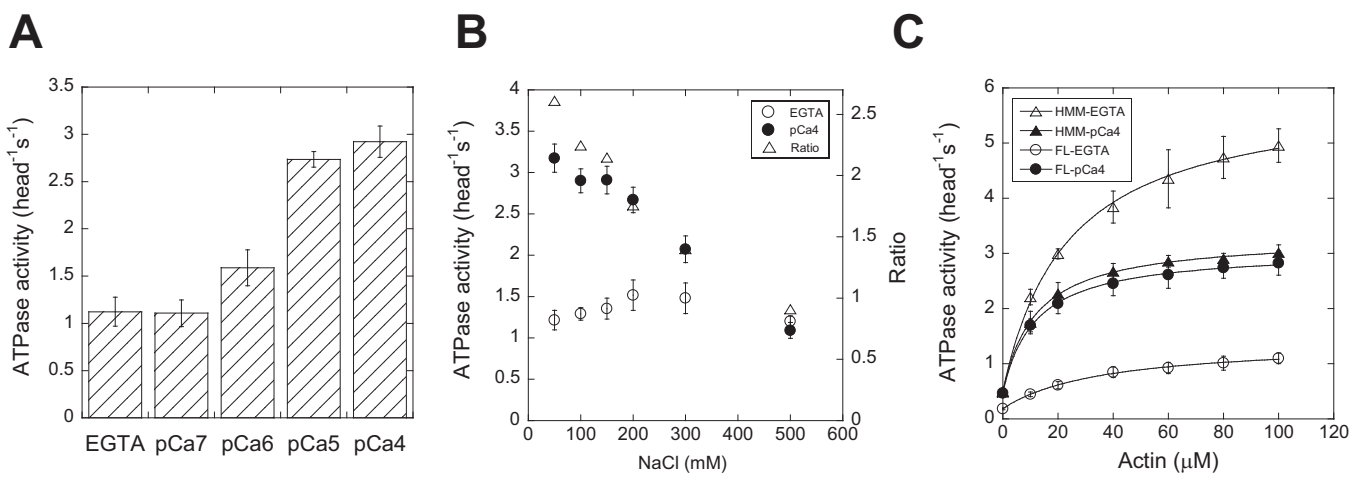

Figure 2 Effects of Ca^{2+} on the ATPase activity of DmM5

(**A**) Effects of various concentrations of free Ca^{2+} on the ATPase activity of DmM5-FL. The ATPase activity was measured as described in the Experimental section, except that 50 mM NaCl and ~0.15 μM DmM5-FL were used. (**B**) Ionic strength dependence of DmM5 ATPase activity in EGTA (open circles) and pCa4 (closed circles) conditions. Open triangles, the ratio of ATPase activity in pCa4 and EGTA conditions. (**C**) Actin dependence of DmM5-FL and DmM5-HMM ATPase activity under EGTA (open circles or triangles) and pCa4 (closed circles or triangles) conditions. The ATPase activity was measured as described above except that ~0.1 μM DmM5-HMM and various concentrations of actin were used. The data were fitted to hyperbola $V = V_0 + V_{max} \times [actin]/(K_{actin} + [actin])$, where V_0 is the ATPase activity in the absence of actin, V_{max} is the maximal actin-activated ATPase activity, and K_{actin} is the concentration of actin that simulates the ATPase activity to 50% of V_{max}. V_0, V_{max} and K_{actin} from multiple assays are summarized in Table 1. Values are means ± S.D. from three or four independent assays.

affinity for actin (K_{actin}) of DmM5-FL ATPase were affected by Ca^{2+}. Ca^{2+} increased the V_{max} from 1.26 ± 0.19 head^{-1}·s^{-1} to 2.59 ± 0.27 head^{-1}·s^{-1} and decreased K_{actin} from 40.9 ± 17.1 μM to 11.8 ± 1.9 μM.

In contrast with DmM5-FL, DmM5-HMM showed high ATPase activity in both EGTA and pCa4 conditions (Figure 2C; Table 1). In EGTA conditions, the V_{max} of ATPase activity of DmM5-HMM (5.45 ± 0.70 head^{-1}·s^{-1}) was ~4.3-fold that of DmM5-FL (1.26 ±0.19 head^{-1}·s^{-1}). In pCa4 conditions, the V_{max} of ATPase activity of DmM5-HMM (2.83 ± 0.14 head^{-1}·s^{-1}) was similar to that of DmM5-FL (2.59 ± 0.27 head^{-1}·s^{-1}). These results indicate that, similar to vertebrate Myo5a, the ATPase activity of DmM5-FL is inhibited by its tail domain and this inhibition is relieved by Ca^{2+}.

We noticed that, unlike vertebrate Myo5a-HMM [4,7], the ATPase activity of DmM5-HMM in pCa4 conditions was substantially lower than that in EGTA conditions (Figure 2C; Table 1). To determine whether the relatively low activity of DmM5-HMM in Ca^{2+} conditions is due to an effect on the ATPase active site in the motor domain or on the dCaM, we measured the ATPase activity of DmM5-motor (containing the motor domain only) and DmM5-1IQ (containing the motor domain and IQ1) in EGTA and pCa4 conditions. Ca^{2+} did not affect the ATPase activity of DmM5-motor, but substantially inhibited that of DmM5-1IQ (Figure 3A), suggesting that the dCaM bound to IQ1 is responsible for the relatively low activity of DmM5-HMM and DmM5-1IQ in pCa4 conditions. To determine whether Ca^{2+} induces dCaM to dissociate from IQ1, thus decreasing the ATPase activity, we quantified the association of DmM5-1IQ with dCaM in EGTA and pCa4 conditions. DmM5-1IQ was constantly associated with a stoichiometric amount of dCaM in both conditions (Figure 3B). In addition, we found that the ATPase activity of DmM5-1IQ, in EGTA or pCa4 conditions, was not significantly affected by exogenous dCaM (Figure 3C). These results indicate that the depression of the ATPase activity of DmM5-1IQ and HMM by Ca^{2+} is not due to the dissociation of dCaM from IQ1 but rather a Ca^{2+}-induced conformational change of dCaM bound to IQ1.

Taken together, these results show that Ca^{2+} has dual effects on the motor function of DmM5, i.e. to activate the motor function

© 2015 Authors; published by Portland Press Limited

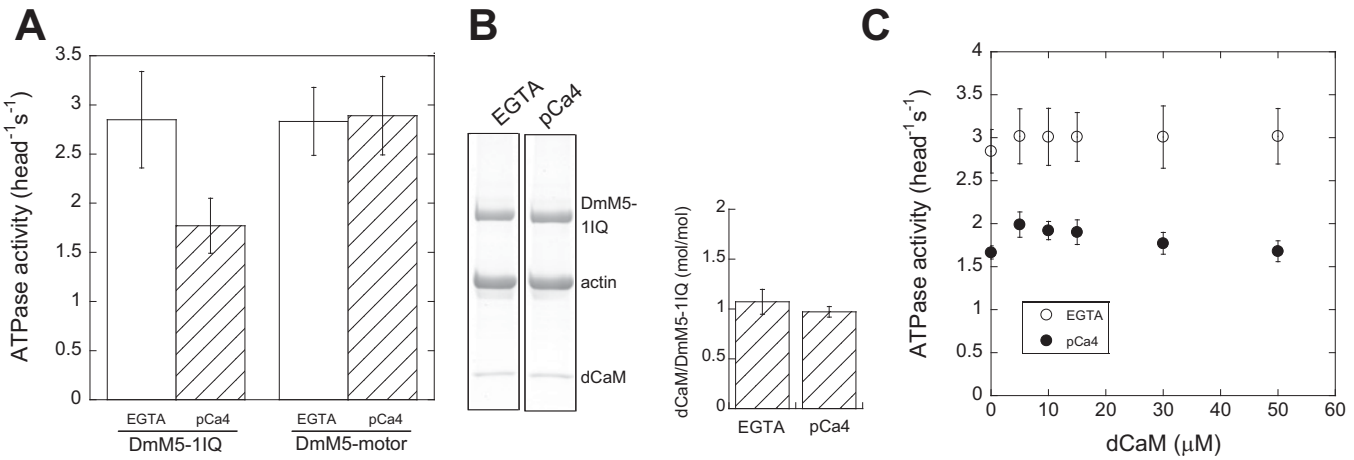

Figure 3 Ca^{2+} inhibits the ATPase activity of DmM5-1IQ

(**A**) Effects of Ca^{2+} on the ATPase activity of DmM5-1IQ and DmM5-motor. The ATPase activity was performed in the presence of 50 mM NaCl and 80 μM actin. (**B**) DmM5-1IQ constantly associates with stoichiometric dCaM in EGTA and pCa4 conditions. DmM5-1IQ (1.6 μM) was incubated with 8 μM actin in 80 μl of 20 mM MOPS/KOH (pH 7.0), 100 mM NaCl, 1 mM $MgCl_2$ and 1 mM EGTA or 100 μM $CaCl_2$ on ice for 10 min. The solution was centrifuged at 418000 ***g*** for 15 min. The pellets were resuspended in ~50 μl of 5 mM EGTA in 1× SDS/PAGE loading buffer, subjected to SDS/PAGE and visualized by Coomassie Brilliant Blue staining (left). dCaM and the heavy chain were quantified with ImageJ software and the molar ratio of dCaM compared with the heavy chain was calculated based on the corresponding molecular masses (right). (**C**) Effects of exogenous dCaM on the ATPase activity of DmM5-1IQ in EGTA and pCa4 conditions. The ATPase activity was measured as described in the Experimental section, except using 50 mM NaCl at the indicated concentration of dCaM and omitting Mlc-C.

by relieving the tail inhibition on the motor domain and to inhibit the motor function by inducing a conformational change of the dCaM bound to IQ1.

dRab11 stimulates the ATPase activity of DmM5

DmM5 plays two distinct roles in the *Drosophila* compound eye: to transport pigment granules and to transport rhodopsin-bearing vesicles [12–14]. DmM5 associates with pigment granules and rhodopsin-bearing vesicles via the cargo-binding proteins Ltd and dRab11 respectively [12,13]. It has been shown that melanophilin, the cargo-binding protein of mouse Myo5a in melanosomes, is able to activate the ATPase activity of Myo5a [10]. We expected that dRab11 and Ltd might be able to activate the ATPase activity of DmM5. To test this possibility, we measured the ATPase activity of DmM5 in the presence of dRab11 or Ltd.

GST-tagged dRab11 was overexpressed in *E. coli* and purified by affinity chromatography (Figure 4A). dRab11 is a small GTPase which switches between the inactive GDP-bound form and the active GTP-bound form. As shown in Figure 4(B), the ATPase activity of DmM5-FL in EGTA conditions was substantially stimulated by 5 μM GTP-bound dRab11, but only marginally stimulated by 5 μM GDP-bound dRab11. It should be mentioned that no significant ATPase activity was detected in the dRab11 sample alone.

dRab11 activated the ATPase activity of DmM5 over a wide range of ionic conditions, but the ratio of the ATPase activity in the presence and absence of dRab11 reached the maximum at 150–200 mM NaCl (Figure 5A). Therefore, we characterized the activation of DmM5 ATPase activity by dRab11 in the presence of 200 mM NaCl in EGTA conditions. As shown in Figure 5(B), the activation of DmM5-FL's ATPase activity by dRab11 followed the Michaelis–Menten equation, with a V_{max} of 1.64 ± 0.19 head$^{-1}\cdot$s^{-1} and an apparent affinity (K_m) of 6.60 ± 2.38 μM dRab11. The maximal ATPase activity of DmM5-FL in the presence of dRab11 was approximately twice that in the absence of dRab11.

To determine whether the activation of DmM5-FL ATPase activity by dRab11 is due to an effect on the maximal ATPase activity (V_{max}) or on the affinity to actin (K_{actin}), we measured the ATPase activity of DmM5-FL with or without 15 μM dRab11 as a function of actin in the presence of 200 mM NaCl. The steady-state V_{max} of DmM5-FL was 2.12 ± 0.37 head$^{-1}\cdot$s^{-1} with a K_{actin} of 134.71 ± 36.39 μM in the absence of dRab11 and was 4.34 ± 0.18 head$^{-1}\cdot$s^{-1} with K_{actin} of 104.62 ± 17.55 μM in the presence of 15 μM dRab11 (Figure 5C; Table 1). These results indicate that the activation of DmM5-FL ATPase activity by dRab11 is largely due to an effect on the maximal ATPase activity.

Because the K_d of dRab11's association with DmM5-FL was 6.6 μM, only 69.4 % of DmM5-FL was stimulated by 15 μM dRab11 [equal to $15/(6.6+15)$]. Thus we expected that the maximal actin-activated ATPase activity of DmM5-FL in the presence of saturating dRab11 is ~6.25 head$^{-1}\cdot$s^{-1} (equal to 4.34 head$^{-1}\cdot$s^{-1}/69.4 %). Under the same conditions, i.e. in the presence of 200 mM NaCl in EGTA conditions, the maximal actin-activated ATPase activity of DmM5-HMM was 5.75 ± 0.79 head$^{-1}\cdot$s^{-1} (Table 1), which is very close to the value for DmM5-FL in the presence of saturating dRab11. These results indicate that dRab11 is able to fully activate DmM5-FL.

DmM5, dRab11 and dRip11 could form a ternary protein complex [13]. To determine whether dRip11 also plays a role in activating DmM5 ATPase activity, we purified Flag-tagged dRip11 expressed in Sf9 cells (Figure 4A) and examined its effect on DmM5-FL ATPase activity. As shown in Figure 4(B), dRip11 did not significantly affect the ATPase activity of DmM5-FL in the absence or presence of dRab11.

Another cargo-binding protein of DmM5 in *Drosophila* compound eye is Ltd, which couples DmM5 to pigment granules [12]. We expressed Flag-tagged Ltd in Sf9 cells and obtained purified protein using affinity chromatography (Figure 4A). To examine whether Ltd is able to activate the motor function of DmM5, we measured the ATPase activity of DmM5-FL in the presence of Ltd under similar conditions to those for dRab11. We found that, unlike dRab11, Ltd did not significantly affect the ATPase activity of DmM5-FL (Figure 4B). It has been shown by yeast two-hybrid analysis and immunoprecipitation

© 2015 Authors; published by Portland Press Limited

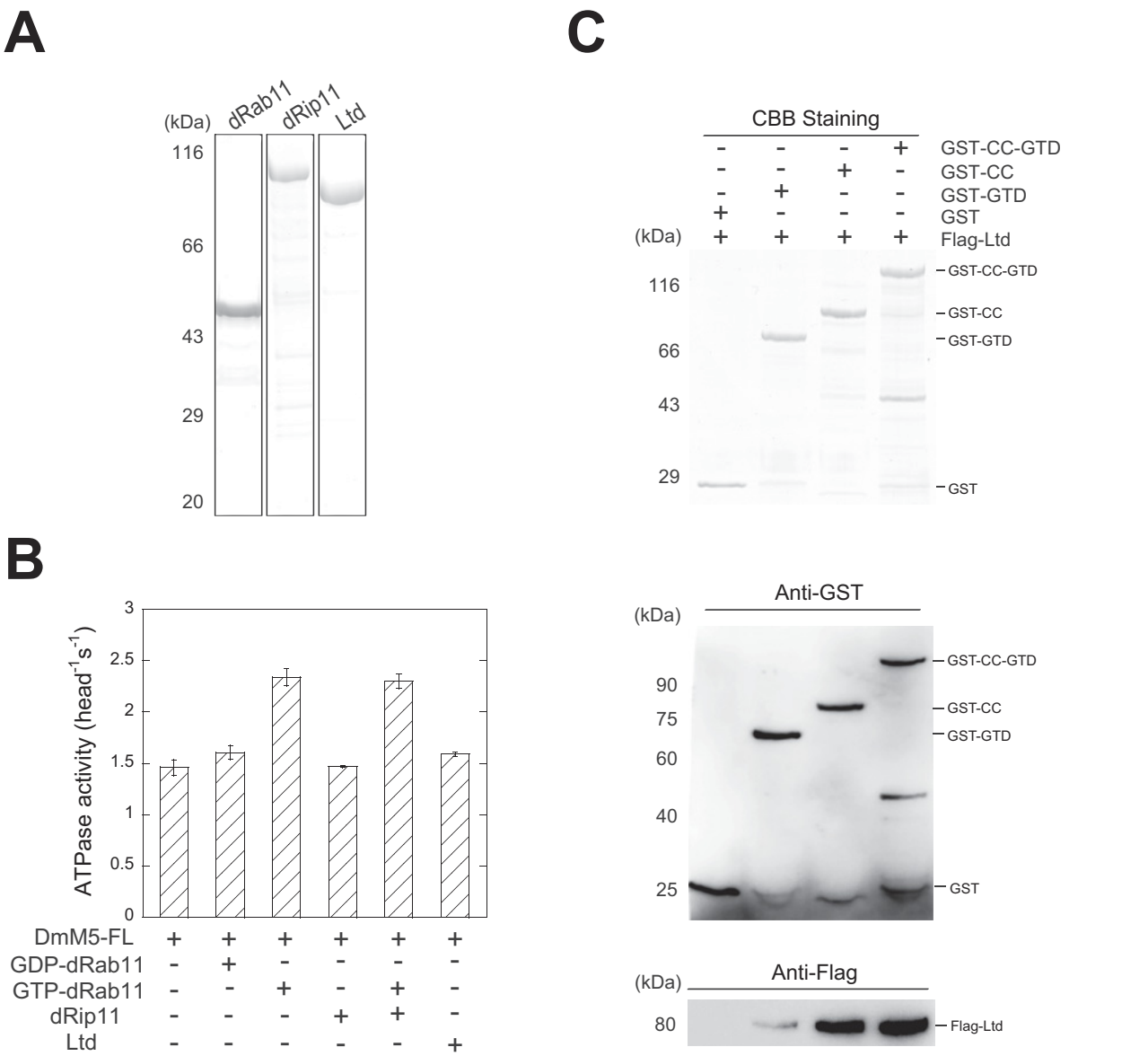

Figure 4 Effects of DmM5-associated proteins on DmM5-FL ATPase activity

(**A**) SDS/PAGE of purified DmM5-associated proteins. (**B**) Effects of DmM5-associated proteins on the ATPase activity of DmM5-FL in EGTA conditions. The assay was conducted as described in the Experimental section, except including 5 μM dRab11, 5 μM Ltd or 1 μM dRip11. (**C**) GST pull-down of GST–DmM5 constructs with Flag–Ltd. The pulled down samples were analysed by SDS/PAGE and detected by Coomassie Brilliant Blue (CBB) staining and Western blot analysis using anti-GST or anti-Flag antibody.

that Ltd interacts with the tail of DmM5 [12]. To confirm and further characterize the interaction between Ltd and DmM5, we performed pull-down assay of Flag-tagged Ltd with GST-tagged DmM5 tail domain constructs. As shown in Figure 4(C), GST–CC–GTD and GST–CC strongly associated with Flag–Ltd, whereas GST–GTD weakly associated with Flag–Ltd, indicating that the CC regions of DmM5 play a dominant role in binding with DmM5. Taken together, these results indicate that Ltd is able to bind to the tail of DmM5 but unable to activate the motor function of DmM5.

dRab11 stimulates the ATPase activity of DmM5 through the GTD

To identify the dRab11-binding site in DmM5, we performed actin co-sedimentation of dRab11 in the presence of DmM5 constructs. As shown in Supplementary Figure S1, dRab11 was co-sedimentated with DmM5-FL but not with DmM5-HMM and DmM5-ΔT, suggesting that the GTD is the binding site for dRab11. To test the direct interaction between the GTD and dRab11, we performed GST pull-down of GST–GTD with Flag–dRab11. A significant amount of Flag–dRab11was pulled down with GST–GTD, but not with GST (the first two lanes in Figure 6A), indicating a direct interaction between dRab11 and the GTD. This result is consistent with the recently solved crystal structure of human Myo5b-GTD in complex with Rab11 (the vertebrate homologue of dRab11) [17], which shows a direct binding of Rab11 to Myo5b-GTD.

Sequence comparison showed that the Rab11-binding site in the GTD of DmM5 is highly homologous to that in the GTD of Myo5b (Supplementary Figure S2A). Thus, we expected a

© 2015 Authors; published by Portland Press Limited

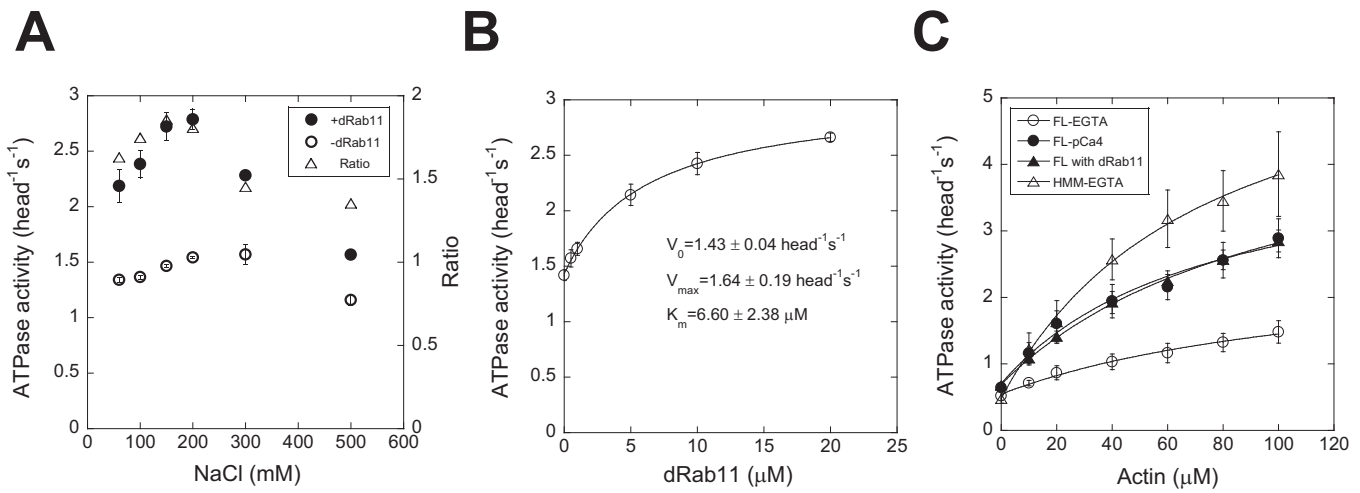

Figure 5 dRab11 stimulates the ATPase activity of DmM5-FL

(**A**) Ionic strength dependence of DmM5-FL ATPase activity in EGTA conditions in the absence (open circles) or presence (closed circles) of 15 μM dRab11. Open triangles, the ratio of ATPase activity in the presence and absence of dRab11. (**B**) Effect of dRab11 on the ATPase activity of DmM5-FL in EGTA conditions. The data were fitted to hyperbola $V = V_0 + V_{max} \times$ [dRab11]/(K_m + [dRab11]), where V_0 is the ATPase activity in the absence of dRab11, V_{max} is the maximal activated ATPase activity by dRab11, and K_m is the concentration of dRab11 that simulates the ATPase activity to 50 % of V_{max}. (**C**) Actin dependence of DmM5-FL ATPase activity in the absence or presence of dRab11. The ATPase assay was conducted in pCa4 conditions or EGTA conditions with or without 15 μM dRab11. The data were fitted to hyperbola to define V_0, V_{max} and K_{actin}. All data are means ± S.D. from three or four independent assays. V_0, V_{max} and K_{actin} from multiple assays are summarized in Table 1. The ATPase assay in (**B**) and (**C**) was conducted in the presence of 200 mM NaCl.

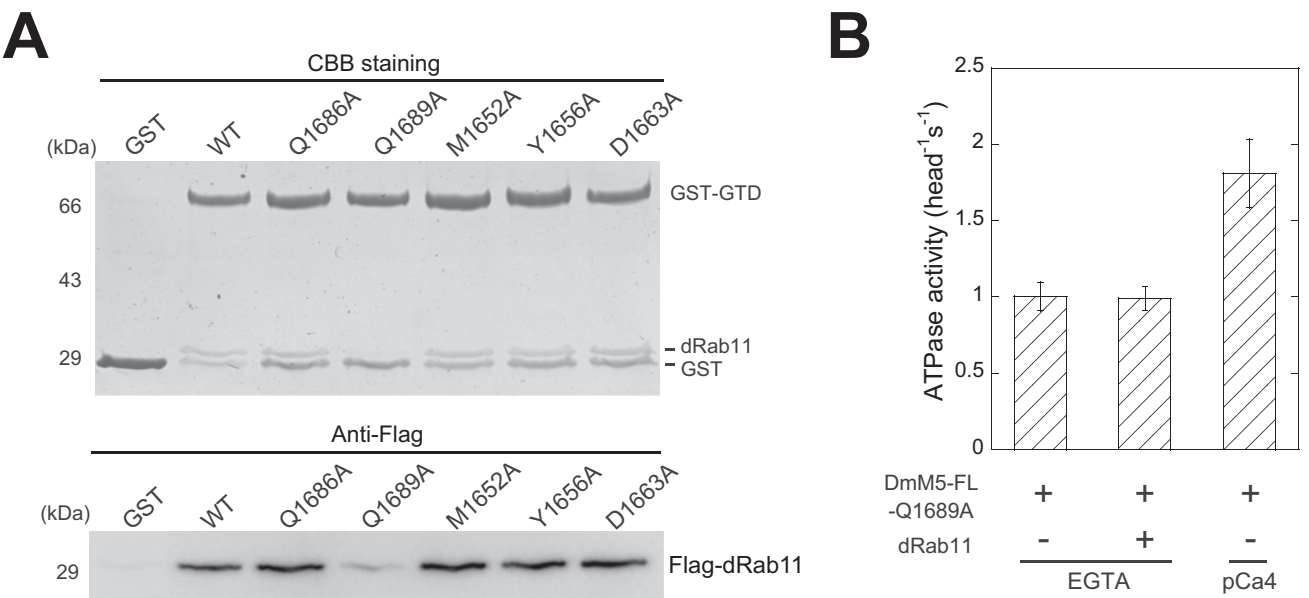

Figure 6 Identification of the key residues in the GTD for the interaction with dRab11

(**A**) GST pull-down of GST-tagged GTD with GTPγS–dRab11. Flag-tagged GTPγS–dRab11 was incubated with GST-tagged GTD wild-type or mutants and subjected to GST pull-down assay. The pulled down samples were analysed by SDS/PAGE and visualized by Coomassie Blue staining (upper) or Western blot analysis using anti-Flag antibody (lower). (**B**) The Q1689A mutation abolishes the activation of DmM5-FL ATPase by dRab11. The ATPase activity was measured in the presence of 80 μM actin in EGTA or pCa4 conditions with or without 5 μM dRab11.

similar interaction between DmM5-GTD and dRab11. There are several conserved residues in the Rab11-binding site in the GTD, including Met^{1652}, Tyr^{1656}, Asp^{1663}, Gln^{1686} and Gln^{1689} (based on the DmM5 sequence). To test the role of these conserved residues in Rab11-binding, we mutated them into alanine individually. GST pull-down of GST–GTD with Flag–dRab11 showed that, among five single amino acid mutations in the GTD, only Q1689A abolished the interaction with dRab11 (Figure 6A). In the crystal structure of the Myo5b-GTD–Rab11 complex, the side chain of Gln^{1748} (corresponding to Gln^{1689} in DmM5) forms hydrogen bonds with Val^{46} and Ile^{76} of Rab11 (Supplementary Figure S2B). The present results indicate that Gln^{1689} is essential for the interaction with dRab11. We therefore expected the Q1689A mutation to abolish the activation of DmM5 ATPase activity by dRab11. As expected, the ATPase activity of DmM5-FL-Q1689A was not significantly stimulated by dRab11 (Figure 6B). On the other hand, similar to that of wild-type, the ATPase activity of DmM5-FL-Q1689A was stimulated by Ca^{2+} (Figure 6B),

© 2015 Authors; published by Portland Press Limited

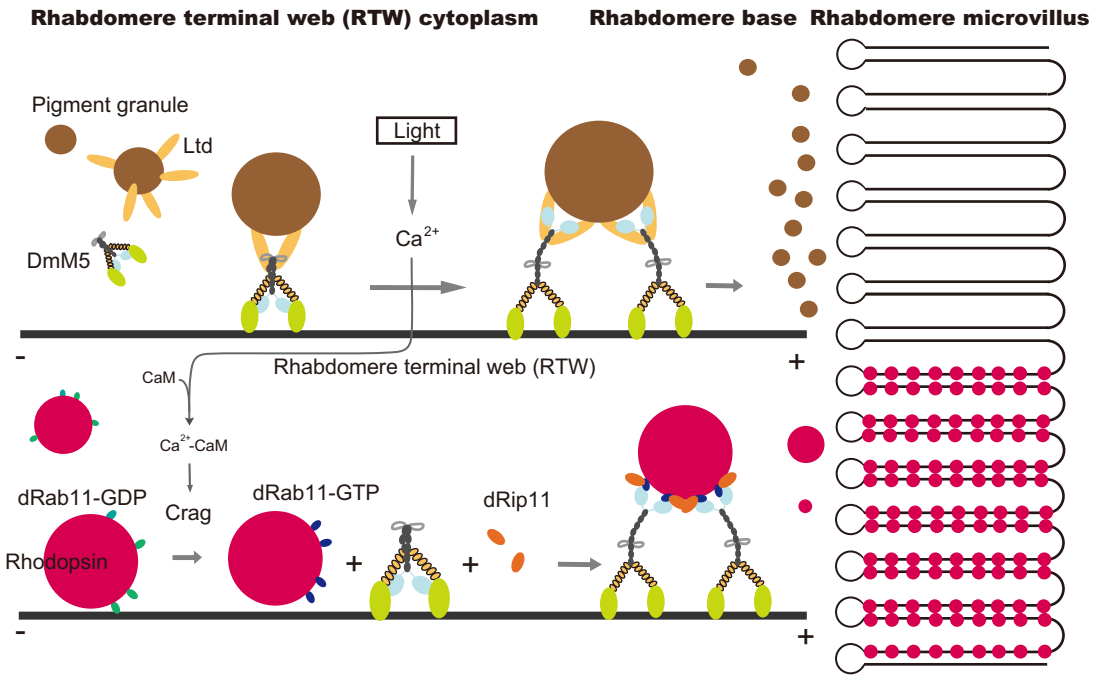

Figure 7 Model for the activation of DmM5 motor functions in *Drosophila* photoreceptor

DmM5 plays two distinct roles in *Drosophila* photoreceptors, i.e. to transport pigment granules and to transport rhodopsin-contained vesicles. The DmM5-dependent transport of pigment granules is directly activated by light-induced Ca^{2+} influx. In dark-adapted photoreceptors, DmM5 associates pigment granules, but its motor function is not activated. Upon illumination, the motor function of DmM5 is activated by the light-induced Ca^{2+} influx and pigment granules are transported along the RTW to the rhabdomere base, thus reducing light exposure. On the other hand, the DmM5-dependent transport of rhodopsin-bearing vesicles is activated by dRab11–GTP. Upon illumination, Ca^{2+} influx activates the GDP/GTP exchange factor of Rab11, Crag. The activated Crag promotes the formation of active GTP–dRab11, which activates the motor function of DmM5. Thus, the rhodopsin-contained secretory vesicles are pulled through the RTW cytoplasm by a DmM5–dRab11 complex to the rhabdomere base.

indicating that the overall structure and the inhibitory function of the GTD was not altered by the Q1689A mutation.

DISCUSSION

Regulation of the motor function of DmM5 by Ca^{2+}

It is well-established that the motor function of vertebrate Myo5 is regulated by Ca^{2+} [4,7,8]. In the present study, we demonstrated that, similar to that of vertebrate Myo5, the motor function of DmM5 is activated by micromolar concentration of Ca^{2+}. The concentration of Ca^{2+} needed to stimulate DmM5 is consistent with the concentration which triggers pigment transport upon illumination in fly compound eye, suggesting that light-induced pigment granule transport in the *Drosophila* compound eye is probably due to Ca^{2+}-induced activation of DmM5.

Although both DmM5 and vertebrate Myo5a ATPase activities are activated by Ca^{2+}, there is a clear difference. The ATPase activity of DmM5-FL in Ca^{2+} conditions is substantially lower than that of the DmM5-HMM in EGTA conditions, whereas that of full-length vertebrate Myo5a in Ca^{2+} conditions is roughly equal to that of Myo5a-HMM in EGTA conditions [4,7]. This discrepancy can be attributed to the different effect of Ca^{2+} on CaM in IQ1 of DmM5 and vertebrate Myo5a. Ca^{2+} substantially inhibits the ATPase activity of truncated DmM5 containing the motor domain and IQ1 (Figure 3A), but has no effect on that of truncated Myo5a containing the motor domain and IQ1 [24,25]. Crystal structure of vertebrate Myo5a shows a direct interaction between the light chain and the converter of the motor domain [26,27]. Thus, it is possible that Ca^{2+} binding to dCaM bound to IQ1 will alter the interaction between dCaM and the motor domain, thus affecting the motor function.

Regulation of the motor function of DmM5 by cargo-binding protein

The tail domain of Myo5 not only acts as an inhibitor of the motor function of the motor domain, but also serves as the binding site for the cargo-binding proteins. It was proposed that cargo-binding proteins of Myo5 might interfere with the interaction between the tail domain and the motor domain, thus activating the function of the motor domain [8]. Although this hypothesis is very attractive as it provides a mechanism to avoid energy waste and enhance the efficiency of intracellular transport, there has been little evidence supporting it. Before the present work, the only evidence directly supporting this hypothesis is the activation of mouse Myo5a by melanophilin [10,28]. In the present study, we have provided further evidence by showing that the DmM5-binding protein dRab11 is capable of activating the motor function of DmM5. Given the high homology between DmM5 and vertebrate Myo5b, as well as that between dRab11 and vertebrate Rab11, it is likely that vertebrate Rab11 is capable of activating the motor function of vertebrate Myo5b.

At present, the mechanism by which dRab11 attenuates the inhibition of the motor domain by the GTD is not known. We propose two possible mechanisms. The first is that dRab11 binding sterically blocks the interaction between the GTD and the head of DmM5. In the crystal structure of human Myo5b-GTD in a complex with Rab11, Rab11 binds on one side of subdomain-2 of vertebrate Myo5b-GTD [17]. Although the precise binding site for the motor domain in the GTD is not known, several structural

© 2015 Authors; published by Portland Press Limited

and functional studies indicate that the motor domain-binding site is also located in subdomain-2 of the GTD [6,29]. Therefore, it is possible that the binding sites for dRab11 and the motor domain in the GTD are partially overlapped and dRab11binding prevents the GTD from binding to the motor domain. The second possible mechanism is that dRab11 allosterically inhibits the interaction between the GTD and the head of DmM5. In other words, dRab11 binding alters the GTD conformation, such that the GTD cannot interact with the head. Further experiments are needed to clarify this issue.

The two functions of DmM5 in the *Drosophila* photoreceptor are probably regulated by different mechanisms

DmM5 plays two distinct roles in the *Drosophila* compound eye photoreceptor, i.e. transport of pigment granules and transport of rhodopsin-bearing vesicles. The former is essential for controlling light exposure in *Drosophila* compound eye photoreceptors [12] and the latter is essential for replenishing the degraded rhodopsin in the rhabdomere base during light exposure [14–16,30,31]. Both processes are stimulated by light exposure, but their kinetics are different. The transport of pigment granules to the rhabdomere base to reduce light exposure is a very rapid and transient process, whereas the transport of rhodopsin-bearing vesicles to replenish the degraded rhodopsin in the rhabdomere base is a continuous and slow process. Therefore, these two processes are probably regulated by different mechanisms.

We propose that the DmM5-dependent transport of pigment granules to the rhabdomere base is directly stimulated by light-induced Ca^{2+} influx (Figure 7). In dark-adapted photoreceptors, DmM5 associates with pigment granules through Ltd. Ltd binds to the CC region of DmM5 and this binding does not activate the motor function of DmM5. Upon illumination, the motor function of DmM5 is activated by light-induced elevation of Ca^{2+} and pigment granules are transported along the exclusionary rhabdomere terminal web (RTW) to the rhabdomere base, thus reducing light exposure. Upon light removal, the Ca^{2+} concentration returns to the resting level, the motor function of DmM5 is inhibited and pigment granules are transported back to the cytosol by an unknown mechanism, thus increasing light exposure.

On the other hand, we propose that the DmM5-dependent transport of rhodopsin-bearing vesicles to the rhabdomere base is activated by GTP-bound dRab11 (Figure 7). It is reported that the GDP/GTP exchange of Rab11 is catalysed by Crag, a guanine-nucleotide-exchange factor (GEF) for dRab11 and the GEF activity of Crag is stimulated by CaM in a Ca^{2+}-dependent manner [16,32]. We therefore propose the following signalling pathway for light-induced transportation of rhodopsin-bearing vesicles from the cytosol to the rhabdomere base. Light-induced Ca^{2+} influx activates CaM which in turn activates Crag's GEF activity. The activated Crag then facilitates the formation of the active GTP-bound Rab11 which in turn binds to DmM5 and activates its motor function. Finally the activated DmM5 starts to pull rhodopsin-bearing vesicles through the RTW to the rhabdomere base. Since the intrinsic GTPase activity of Rab11 is very low, the long-lived GTP-bound dRab11 would ensure a continual replenishment of rhodopsin in the rhabdomere base even after light exposure.

AUTHOR CONTRIBUTION

Huan-Hong Ji was the primary person responsible for performing the experiments of the present study. Hai-Man Zhang, Mei Shen and Lin-Lin Yao contributed to the experimental work. Huan-Hong Ji and Xiang-dong Li designed the experiments, analysed the data and wrote the manuscript.

ACKNOWLEDGEMENTS

We thank Dr Paul Odgren (University of Massachusetts Medical School) for reading the manuscript before submission.

FUNDING

This work was supported by the National Basic Research Program of China [grant numbers 2012CB114102 and 2013CB932802]; the National Natural Science Foundation of China [grant numbers 31171367 and 31470791]; and the State Key Laboratory of Integrated Management of Pest Insects and Rodents [grant number IPM1416].

REFERENCES

1 Woolner, S. and Bement, W.M. (2009) Unconventional myosins acting unconventionally. Trends Cell Biol. **19**, 245–252 CrossRef PubMed
2 Hammer, J.A. and Sellers, J.R. (2011) Walking to work: roles for class V myosins as cargo transporters. Nat. Rev. Mol. Cell Biol. **13**, 13–26 PubMed
3 Tóth, J., Kovács, M., Wang, F., Nyitray, L. and Sellers, J.R. (2005) Myosin V from *Drosophila* reveals diversity of motor mechanisms within the myosin V family. J. Biol. Chem. **280**, 30594–30603 CrossRef PubMed
4 Li, X.D., Mabuchi, K., Ikebe, R. and Ikebe, M. (2004) Ca^{2+}-induced activation of ATPase activity of myosin Va is accompanied with a large conformational change. Biochem. Biophys. Res. Commun. **315**, 538–545 CrossRef PubMed
5 Li, X.D., Jung, H.S., Mabuchi, K., Craig, R. and Ikebe, M. (2006) The globular tail domain of myosin Va functions as an inhibitor of the myosin Va motor. J. Biol. Chem. **281**, 21789–21798 CrossRef PubMed
6 Li, X.D., Jung, H.S., Wang, Q., Ikebe, R., Craig, R. and Ikebe, M. (2008) The globular tail domain puts on the brake to stop the ATPase cycle of myosin Va. Proc. Natl. Acad. Sci. U.S.A. **105**, 1140–1145 CrossRef PubMed
7 Krementsov, D.N., Krementsova, E.B. and Trybus, K.M. (2004) Myosin V: regulation by calcium, calmodulin, and the tail domain. J. Cell Biol. **164**, 877–886 CrossRef PubMed
8 Wang, F., Thirumurugan, K., Stafford, W.F., Hammer, J.A., Knight, P.J. and Sellers, J.R. (2004) Regulated conformation of myosin V. J. Biol. Chem. **279**, 2333–2336 CrossRef PubMed
9 Thirumurugan, K., Sakamoto, T., Hammer, J.R., Sellers, J.R. and Knight, P.J. (2006) The cargo-binding domain regulates structure and activity of myosin 5. Nature **442**, 212–215 CrossRef PubMed
10 Li, X.D., Ikebe, R. and Ikebe, M. (2005) Activation of myosin Va function by melanophilin, a specific docking partner of myosin Va. J. Biol. Chem. **280**, 17815–17822 CrossRef PubMed
11 Franceschini, N. and Kirschfeld, K. (1971) Les phénomènes de pseudopupille dans l'œil composé de *Drosophila*. Kybernetik **9**, 159–182 CrossRef PubMed
12 Satoh, A.K., Li, B.X., Xia, H. and Ready, D.F. (2008) Calcium-activated myosin V closes the *Drosophila* pupil. Curr. Biol. **18**, 951–955 CrossRef PubMed
13 Li, B.X., Satoh, A.K. and Ready, D.F. (2007) Myosin V, Rab11, and dRip11 direct apical secretion and cellular morphogenesis in developing *Drosophila* photoreceptors. J. Cell Biol. **177**, 659–669 CrossRef PubMed
14 Pocha, S.M., Shevchenko, A. and Knust, E. (2011) Crumbs regulates rhodopsin transport by interacting with and stabilizing myosin V. J. Cell Biol. **195**, 827–838 CrossRef PubMed
15 Satoh, A.K., O'Tousa, J.E., Ozaki, K. and Ready, D.F. (2005) Rab11 mediates post-Golgi trafficking of rhodopsin to the photosensitive apical membrane of *Drosophila* photoreceptors. Development **132**, 1487–1497 CrossRef PubMed
16 Xiong, B., Bayat, V., Jaiswal, M., Zhang, K., Sandoval, H., Charng, W., Li, T., David, G., Duraine, L., Lin, Y. et al. (2012) Crag is a GEF for Rab11 required for rhodopsin trafficking and maintenance of adult photoreceptor cells. PLoS Biol. **10**, e1001438 CrossRef PubMed
17 Pylypenko, O., Attanda, W., Gauquelin, C., Lahmani, M., Coulibaly, D., Baron, B., Hoos, S., Titus, M.A., England, P. and Houdusse, A.M. (2013) Structural basis of myosin V Rab GTPase-dependent cargo recognition. Proc. Natl. Acad. Sci. U.S.A. **110**, 20443–20448 CrossRef PubMed
18 Lapierre, L.A., Kumar, R., Hales, C.M., Navarre, J., Bhartur, S.G., Burnette, J.O., Provance, D.J., Mercer, J.A., Bahler, M. and Goldenring, J.R. (2001) Myosin vb is associated with plasma membrane recycling systems. Mol. Biol. Cell. **12**, 1843–1857 CrossRef PubMed
19 Spudich, J.A. and Watt, S. (1971) The regulation of rabbit skeletal muscle contraction: I. Biochemical studies of the interaction of the tropomyosin-troponin complex with actin and the proteolytic fragments of myosin. J. Biol. Chem. **246**, 4866–4871 PubMed

© 2015 Authors; published by Portland Press Limited

20 Ma, R.N., Mabuchi, K., Li, J., Lu, Z., Wang, C.L. and Li, X.D. (2013) Cooperation between the two heads of smooth muscle myosin is essential for full activation of the motor function by phosphorylation. Biochemistry **52**, 6240–6248 CrossRef PubMed
21 Cao, Y., White, H.D. and Li, X.D. (2014) Drosophila myosin-XX functions as an actin-binding protein to facilitate the interaction between Zyx102 and actin. Biochemistry **53**, 350–360 CrossRef PubMed
22 Ikebe, M., Reardon, S., Schwonek, J.P., Sanders, C.N. and Ikebe, R. (1994) Structural requirement of the regulatory light chain of smooth muscle myosin as a substrate for myosin light chain kinase. J. Biol. Chem. **269**, 28165–28172 PubMed
23 Lu, Z., Shen, M., Cao, Y., Zhang, H., Yao, L. and Li, X. (2012) Calmodulin bound to the first IQ motif is responsible for calcium-dependent regulation of myosin 5a. J. Biol. Chem. **287**, 16530–16540 CrossRef PubMed
24 Homma, K., Saito, J., Ikebe, R. and Ikebe, M. (2000) Ca^{2+}-dependent regulation of the motor activity of myosin V. J. Biol. Chem. **275**, 34766–34771 CrossRef PubMed
25 Trybus, K.M., Krementsova, E. and Freyzon, Y. (1999) Kinetic characterization of a monomeric unconventional myosin V construct. J. Biol. Chem. **274**, 27448–27456 CrossRef PubMed
26 Coureux, P.D., Wells, A.L., Menetrey, J., Yengo, C.M., Morris, C.A., Sweeney, H.L. and Houdusse, A. (2003) A structural state of the myosin V motor without bound nucleotide. Nature **425**, 419–423 CrossRef PubMed
27 Coureux, P.D., Sweeney, H.L. and Houdusse, A. (2004) Three myosin V structures delineate essential features of chemo-mechanical transduction. EMBO J. **23**, 4527–4537 CrossRef PubMed
28 Sckolnick, M., Krementsova, E.B., Warshaw, D.M. and Trybus, K.M. (2013) More than just a cargo adapter, melanophilin prolongs and slows processive runs of myosin Va. J. Biol. Chem. **288**, 29313–29322 CrossRef PubMed
29 Pashkova, N., Jin, Y., Ramaswamy, S. and Weisman, L.S. (2006) Structural basis for myosin V discrimination between distinct cargoes. EMBO J. **25**, 693–700 CrossRef PubMed
30 Satoh, A.K. and Ready, D.F. (2005) Arrestin1 mediates light-dependent rhodopsin endocytosis and cell survival. Curr. Biol. **15**, 1722–1733 CrossRef PubMed
31 Xiong, B. and Bellen, H.J. (2013) Rhodopsin homeostasis and retinal degeneration: lessons from the fly. Trends Neurosci. **36**, 652–660 CrossRef PubMed
32 Xu, X.Z., Wes, P.D., Chen, H., Li, H.S., Yu, M., Morgan, S., Liu, Y. and Montell, C. (1998) Retinal targets for calmodulin include proteins implicated in synaptic transmission. J. Biol. Chem. **273**, 31297–31307 CrossRef PubMed

Received 21 November 2014/4 May 2015; accepted 5 May 2015
Published as BJ Immediate Publication 5 May 2015, doi:10.1042/BJ20141330

© 2015 Authors; published by Portland Press Limited

Figure S1 (Ji et al)

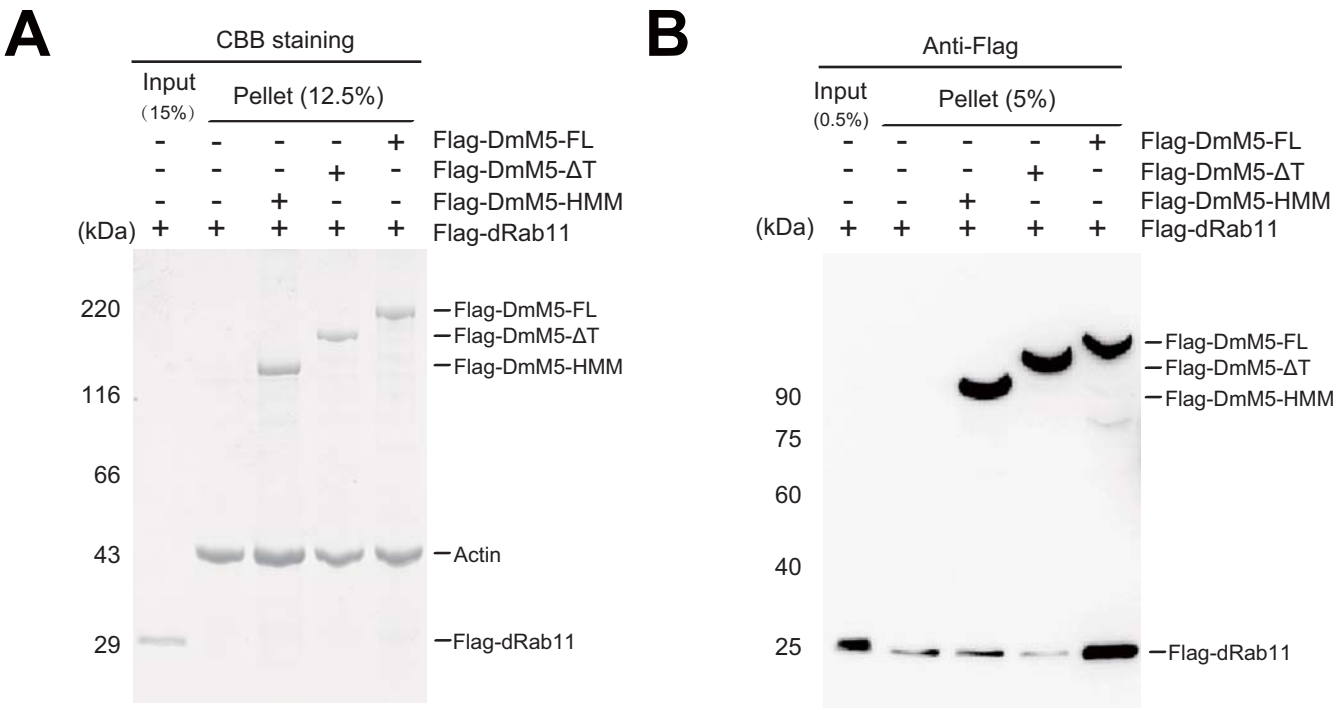

Figure S1. Actin cosedimentation of DmM5 constructs with dRab11. Flag-tagged GTPγS- dRab11 was incubated with actin and Flag-tagged DmM5 constructs and then subjected to ultracentrifugation. The pellets were analyzed by SDS-PAGE and visualized by Coomassie Brilliant Blue staining (A) or Western blot using anti-Flag antibody (B).

Figure S2 (Ji et al)

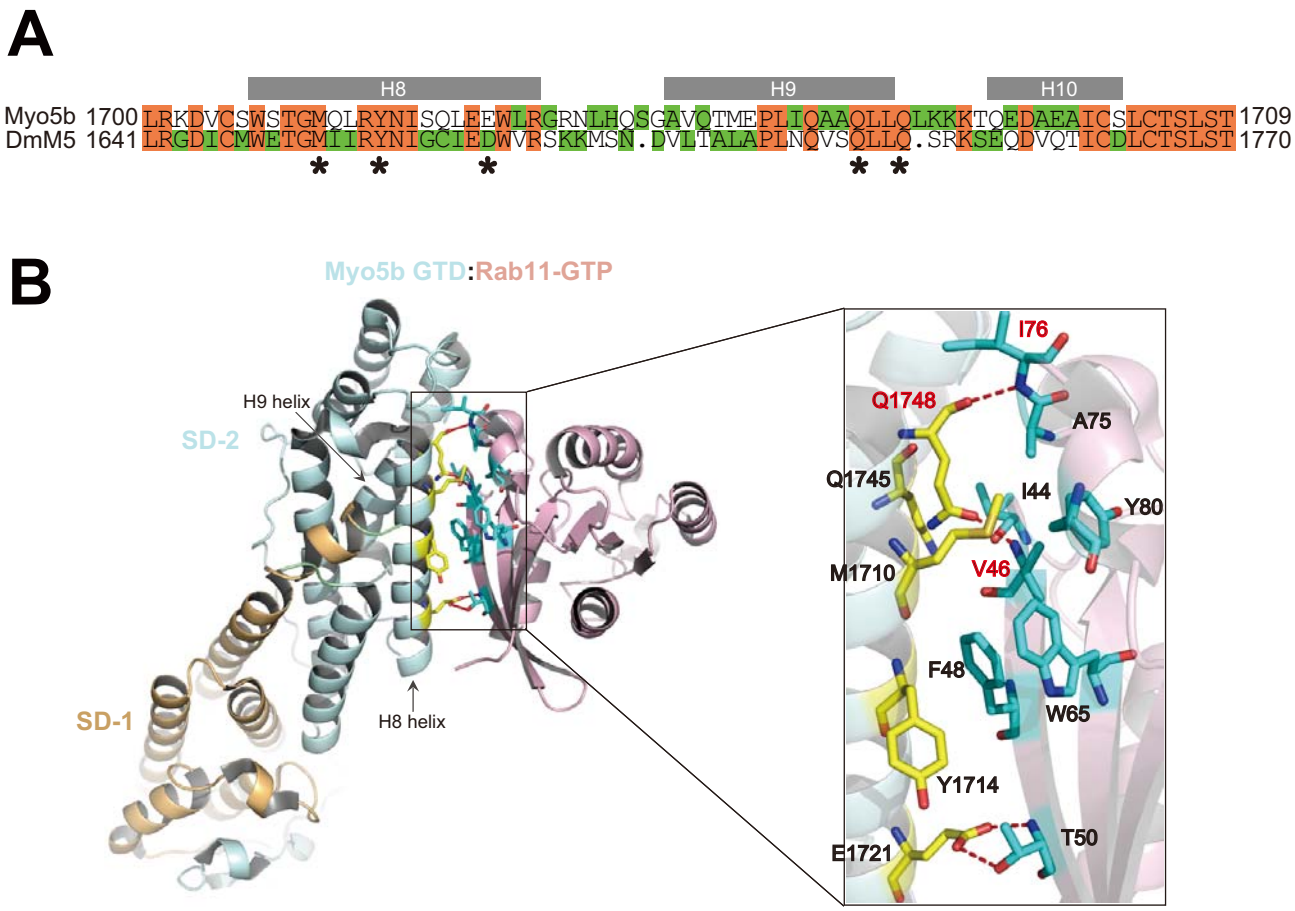

Figure S2. The Rab11-binding site in the GTD is conserved between DmM5 and human Myo5b. (A) Sequence alignment shows the conserved residues in the Rab11-binding site of DmM5 GTD and human Myo5b GTD. The gray bars shown above the alignment indicate α-helixes in the crystal structure of Myo5b GTD. Black stars indicate the mutated residues in this study. (B) The crystal structure of human Myo5b-GTD in complex with Rab11a–GTP (PDB ID: 4LX0). The subdomain-1 (SD-1) and subdomain-2 (SD-2) of Myo5b GTD are highlighted in light orange and pale cyan, respectively. dRab11 is shown in light pink.The conserved residues in the Rab11-binding site of the GTD are labeled in yellow. The residues of Rab11 involved in the interaction with the GTD are labeled in cyan.